Spectroscopic properties of Pr^{3+} ions in lead germanate glass

1999 J. Phys.: Condens. Matter 11 7411

(http://iopscience.iop.org/0953-8984/11/38/317)

J. Phys.: Condens. Matter **11** (1999) 7411–7421. Printed in the UK PII: S0953-8984(99)99933-2

Spectroscopic properties of Pr^{3+} ions in lead germanate glass

R Balda†, J Fernández†, A de Pablos‡ and J M Fdez-Navarro‡

† Departamento de Física Aplicada I, ETSII y Telecom, Universidad del País Vasco, Alameda Urquijo s/n, 48013, Bilbao, Spain

‡ Instituto de Cerámica y Vidrio, Arganda del Rey, Madrid, Spain

Received 4 December 1998, in final form 12 July 1999

Abstract. The visible luminescence of Pr^{3+}-doped lead germanate glass of composition (in mol%) 60PbO–40GeO_2 has been investigated for two Pr^{3+} concentrations at different temperatures by using steady-state and time-resolved laser spectroscopy. Concentration quenching of the $^1D_2$ emission is observed for Pr^{3+} concentrations higher than $x = 0.05$ mol% even at 4.2 K and attributed to a cross relaxation process. Anti-Stokes emission from the $^3P_0$ level following excitation of the $^1D_2$ state has been observed for the sample doped with 0.5 mol% of Pr^{3+}. The temporal behaviour of the anti-Stokes emission from the $^3P_0$ level following excitation of the $^1D_2$ state suggests that energy transfer is responsible for the upconversion process.

1. Introduction

In the last decade, a large amount of research has been carried out to investigate new rare-earth (RE) doped glasses for applications in optical devices of laser technology [1, 2]. Among the different compositions studied to improve the optical properties of RE doped glasses, it was found that germanate glasses have smaller maximum vibrational frequencies than those shown by silicate, phosphate and borate glasses [3, 4]. The reduced phonon energy increases the quantum efficiency of luminescence from excited states of RE ions in these matrices and provides the possibility to develop more efficient lasers and fibre optics amplifiers at longer wavelengths than available from other oxide glasses. Among these, lead germanate glasses are particularly interesting since they can be readily made in fibre form for applications in optoelectronics [5–7].

Trivalent praseodymium is an attractive optical activator which offers the possibility of simultaneous blue, green and red emission for laser action, as well as infrared emission for optical amplification at 1.3 μm [8]. Pr^{3+} systems are also interesting as short-wavelength upconversion laser materials [9–11]. One of the general features of some fluorescing levels of the Pr^{3+} ion is that the emission is quenched when concentration and/or temperature increase. Among the energy transfer mechanisms responsible for this quenching, cross-relaxation and upconversion are very important. Upconversion is particularly interesting since it may lead to the observation of anti-Stokes fluorescence, having many applications in upconversion lasers [12]. In addition, it is a very useful tool in studying the higher energy states of the optically active centres in solids.

In upconversion laser schemes, excitation of the metastable optical states of RE ions is achieved by: (i) sequential absorption of pump photons in one ion involving excited state absorption (ESA), (ii) photon avalanche and (iii) energy transfer upconversion (ETU). In the latter mechanism, two ions excited in an intermediate state in close proximity are coupled

0953-8984/99/387411+11$30.00

by a non-radiative process in which an ion returns to the ground state while the other one is promoted to the upper level. In most cases, the cross relaxation processes are based on electric dipole–dipole interactions [13, 14].

Upconverted blue emission has been observed in borate [15], fluoroindate [16], tellurite [17] and fluorophosphate glasses [18] following orange–yellow excitation. Upconversion is explained for borate, fluoroindate and fluorophosphate glasses in terms of energy transfer, whereas in the case of tellurite glasses a sequential two-photon excitation process is proposed as the dominant mechanism of the upconversion.

The aim of this work is to characterize the properties of the visible luminescence from Pr^{3+} doped lead germanate glass. The study includes absorption, emission, lifetime results and fluorescence quenching of the $^1D_2$ emission. We also present the results of orange to blue upconversion obtained by pumping the $^1D_2$ state. The time evolution of the upconverted fluorescence proves that upconversion occurs via energy transfer.

2. Experimental techniques

Batches of 20 g of glass have been prepared by mixing high purity reagents GeO_2 (Alfa 99.999) and PbO (Alfa 99.9995) and doped with 0.05 and 0.5% Pr_2O_3 (Alfa 99.999). This mixture was melted in a high purity alumina crucible placed in a vertical tubular furnace at temperature between 1100 and 1200 °C for 1 h and then poured onto a preheated brass plate, followed by 1 h annealing at 420 °C and a further cooling at 1.5 °C min^{-1} down to room temperature. Finally the samples were cut and polished for optical measurements.

The sample temperature was varied between 4.2 K and 300 K with a continuous flow cryostat. Conventional absorption spectra were performed with a Cary 5 spectrophotometer. The steady-state emission measurements were made with an argon laser as exciting light. The fluorescence was analysed with a 0.25 monochromator, and the signal was detected by a Hamamatsu R928 photomultiplier and finally amplified by a standard lock-in technique.

Time-resolved fluorescence spectra were performed by exciting the samples with a pulsed frequency doubled Nd:YAG pumped tunable dye laser of 9 ns pulse width and 0.08 cm^{-1} linewidth, and detected by an EGG-PAR optical multichannel analyser. For lifetime measurements, the fluorescence was analysed with a 1 m Spex monochromator, and the signal was detected by a Hamamatsu R928 photomultiplier. Data were processed by an EGG-PAR boxcar integrator.

Emission measurements under excitation in the $^1D_2$ state were performed by using a high power optical parametric oscillator (MOPO, Spectra Physics model 730) which provides 10 ns pulses of about 35 mJ of average energy with a repetition rate of 10 Hz. The luminescence was dispersed by a 500 M Spex monochromator (spectral resolution $\approx$ 0.05 nm) and detected with a cooled photomultiplier. The signals were recorded by using a SR400 two-channel gated photon counter. The decay time measurements were performed with the averaging facilities of a Tektronix 2400 digital storage oscilloscope.

3. Results

3.1. Absorption and emission properties

The room temperature absorption spectra were obtained for both samples in the 350–2500 nm range by making use of a Cary 5 spectrophotometer. As an example figure 1 shows the room temperature absorption spectrum of the sample doped with 0.5 mol% of Pr^{3+} in the 400–2500 nm range. The spectrum consists of several bands corresponding to transitions

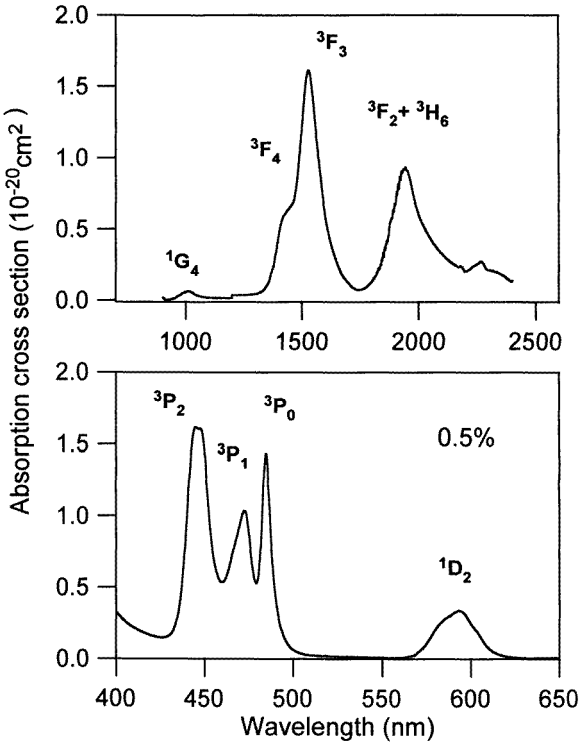

Figure 1. Room temperature absorption spectrum of the sample doped with 0.5 mol% of Pr^{3+} in the 400–2500 nm range.

between the $^3H_4$ ground state and the excited multiplets belonging to the $4f^2$ configuration of Pr^{3+} ions. The high energy group was associated with transitions from the $^3H_4$ state to the $^3P_{0,1,2}$+$^1I_6$ multiplets. The band located at about 590 nm was associated with transitions from the $^3H_4$ ground state to the $^1D_2$ state. In the near infrared the weak band centred at about 1000 nm corresponds to the $^3H_4 \rightarrow {}^1G_4$ spin-forbidden transition, and the bands between 1200 and 2200 nm correspond to transitions to the $^3F_{2,3,4}$ multiplet and $^3H_6$ states. The broad lines are due to large site-to-site variations of the crystal field strengths. Figure 2 shows the simplified energy level diagram showing the positions of the J states of the Pr^{3+} ions in this glass derived from the absorption spectrum. The position of the $^3H_5$ band inferred from the emission spectrum is also included. Table 1 shows the peak positions of the absorption bands of Pr^{3+} ions in this glass at 295 K.

The room temperature steady-state emission spectra were obtained in the 470–800 nm spectral range by exciting with an argon laser. Figure 3 shows the emission spectrum for the sample doped with 0.5 mol% of Pr^{3+}. As can be seen, after excitation in the $^3P_2$ level (454 nm) there is emission from $^3P_0$ and $^1D_2$ levels. The emission lines are related to transitions $^3P_0 \rightarrow {}^3H_{4,5,6}$, $^3P_0 \rightarrow {}^3F_{2,3,4}$ and $^1D_2 \rightarrow {}^3H_{4,5}$. Simultaneous emissions from the $^3P_0 \rightarrow {}^3H_6$ and $^1D_2 \rightarrow {}^3H_4$ transitions are observed in the region between 600 and 630 nm. This is confirmed by the time-resolved emission spectra.

The time evolution of the luminescence from the emitting levels has been investigated by time-resolved spectroscopy. The time-resolved emission spectra in the 470–750 nm range were performed at 77 K by exciting the samples at the $^3H_4 \rightarrow {}^3P_0$ transition and recording

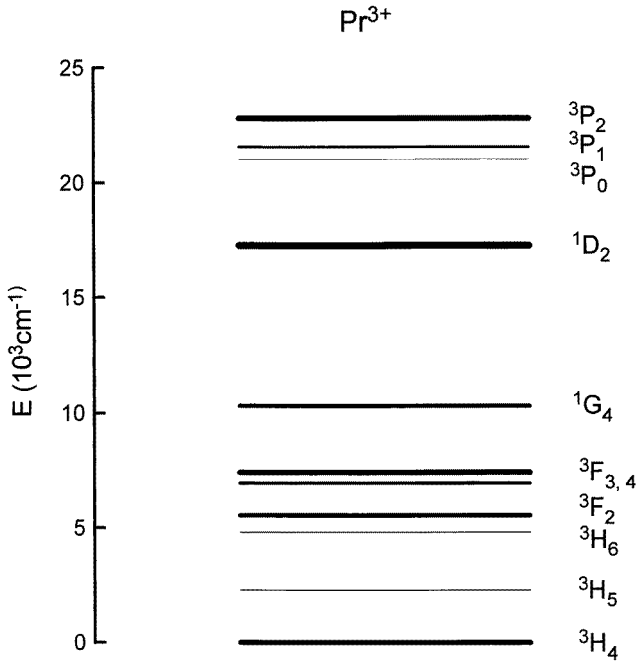

Figure 2. Energy level diagram of Pr^{3+} in lead germanate glass (from the absorption data).

Table 1. Peak positions of the Pr^{3+} absorption bands at 295 K in lead germanate glass.

Transition	Energy (cm^{-1})	Wavelength (nm)
$^3H_4 \rightarrow {}^3P_2$	22 401	446
$^3H_4 \rightarrow {}^3P_1$	21 155	473
$^3H_4 \rightarrow {}^3P_0$	20 623	485
$^3H_4 \rightarrow {}^1D_2$	16 860	593
$^3H_4 \rightarrow {}^1G_4$	9 907	1009
$^3H_4 \rightarrow {}^3F_3 + {}^3F_4$	6 625	1509
$^3H_4 \rightarrow {}^3F_2 + {}^3H_6$	5 042	1983

the luminescence at different time delays after the laser pulse. Figure 4 presents the time-resolved emission spectra for the sample doped with 0.5 mol% of Pr^{3+}. These spectra show the emissions from the $^3P_0$ and $^1D_2$ levels. As can be seen from this figure there is a decrease of the emission of the $^3P_0$ level as time increases from 10 ns to 100 μs. The emission decay of this level is faster than the decay of $^1D_2$ and, as expected, for long time delays only the emissions from state $^1D_2$ remain. This behaviour confirms the existence of simultaneous emissions from the $^1D_2 \rightarrow {}^3H_4$ and $^3P_0 \rightarrow {}^3H_6$ transitions in the region between 600 and 630 nm.

3.2. Lifetime results

In order to obtain additional information about the luminescence properties of Pr^{3+} ions in this glass, the fluorescence dynamics of the $^3P_0$ and $^1D_2$ emitting levels were investigated for both Pr^{3+} concentrations at different temperatures. Decay curves for both concentrations

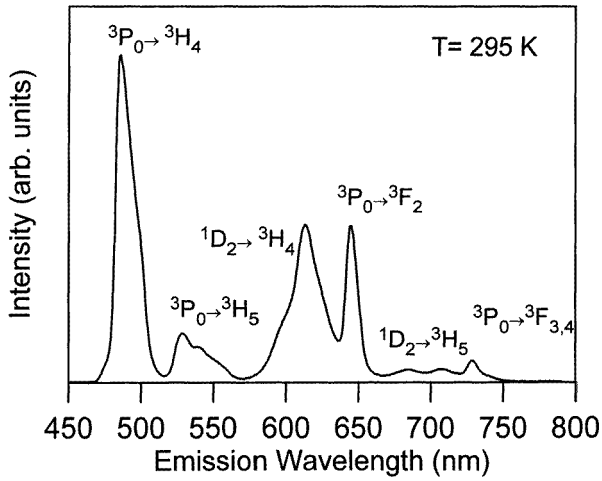

Figure 3. Steady-state emission spectrum of the glass doped with 0.5 mol% of Pr^{3+} obtained at room temperature by exciting the sample at 454 nm.

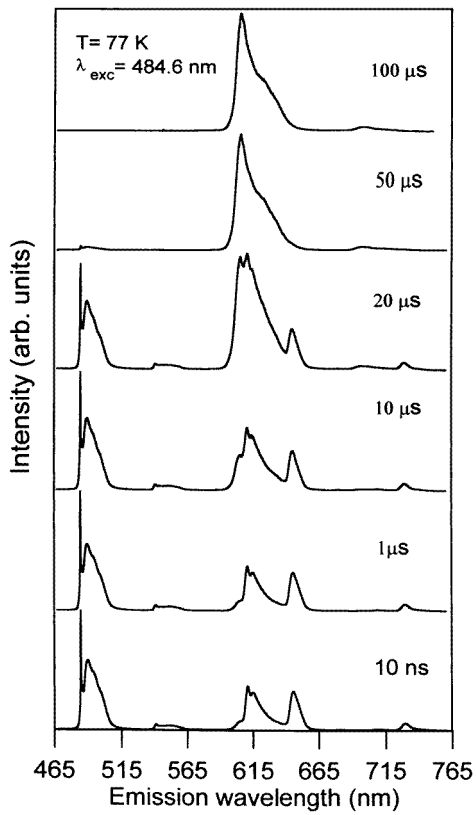

Figure 4. Time-resolved emission spectra obtained at different time delays after the laser pulse between 10 ns and 100 μs for the glass doped with 0.5 mol% of Pr^{3+}. Measurements were performed at 77 K.

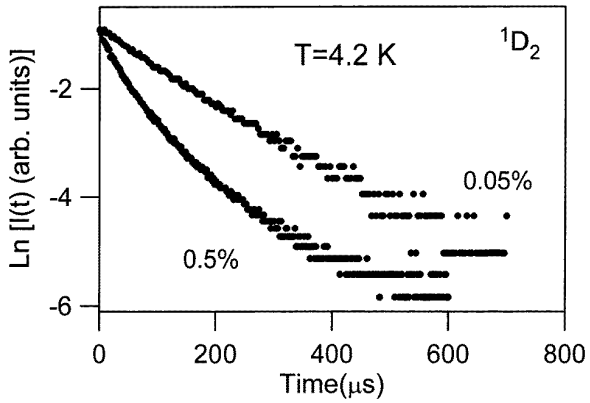

Figure 5. Logarithmic plot of the fluorescence decays of the $^1D_2$ level for samples with 0.05 and 0.5 mol% of Pr^{3+}. The decays were obtained by exciting at the $^3P_0$ level (486 nm) at 4.2 K.

were obtained under laser pulsed excitation at 486 nm, by collecting the luminescence at different emission wavelengths between 490 and 720 nm. The decays of the $^1D_2$ level can be described at low concentration (0.05 mol%) by an exponential function in the 4.2 K–295 K temperature range. As concentration increases the decays become non-exponential and the lifetime decreases from 145 μs for the sample doped with 0.05% to 48 μs (for the non-exponential decay curves we have considered the lifetime τ such as $I(t = \tau) = I_0/e$) for the sample doped with 0.5%. Figure 5 shows, as an example, the logarithmic plot of the experimental decays of the $^1D_2$ level (excited at 486 nm) at 4.2 K for two different concentrations 0.05 and 0.5 mol%. This variation of fluorescence from the $^1D_2$ level with concentration shows the presence of energy transfer processes at concentrations higher than 0.05 mol%. The same behaviour was observed at 77 K and 295 K. However, the decays of the $^3P_0$ level can be described for both concentrations by a single exponential function and the lifetime values (≈ 6 μs) do not change in this concentration range. The lifetimes of the two levels are almost independent of temperature between 4.2 and 300 K.

As in other Pr^{3+} systems investigated [19–21], the $^1D_2$ emission is affected much more strongly by quenching than is $^3P_0$, so we will focus the discussion on the $^1D_2$ level and its fluorescence dynamics.

3.3. Orange to blue frequency upconversion

To investigate the possibility of upconverted fluorescence in this system we have excited directly the $^1D_2$ level and we have observed anti-Stokes fluorescence from the $^3P_0 \rightarrow {}^3H_4$ transition in the 4.2 K–295 K temperature range for the sample doped with 0.5 mol% of Pr^{3+}. Figure 6 shows the upconverted emission spectra for the sample doped with 0.5 mol% at three different temperatures, 4.2, 130 and 295 K obtained by exciting at 590 nm.

The intensity of the anti-Stokes emission shows a quadratic dependence with the excitation laser energy indicating that two photons participate in this process [15–18]. Figure 7 shows a logarithmic plot of the integrated emission intensity of the upconverted fluorescence as a function of the pump laser intensity.

The temporal evolution of the blue emission is illustrated in figure 8 for the sample doped with 0.5 mol%. This figure shows, as an example, the experimental decay of the $^3P_0$ level obtained at 4.2 K by exciting at 486 nm and at 590 nm. As can be observed the decay curve

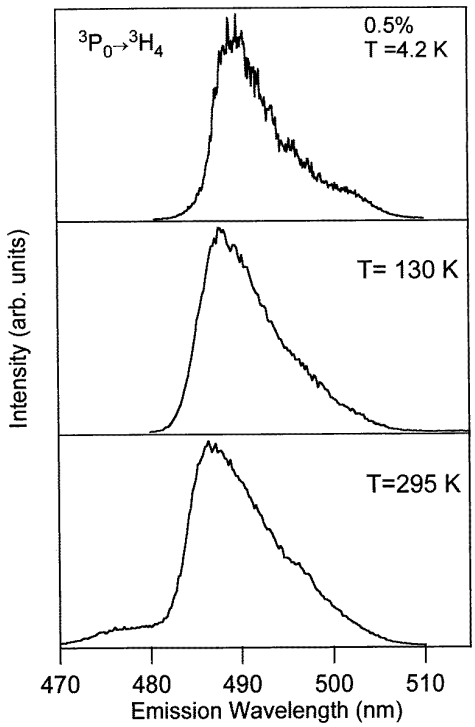

Figure 6. Fluorescence spectrum corresponding to the $^3P_0 \rightarrow {}^3H_4$ transition at three different temperatures. The excitation wavelength (590 nm) was in resonance with the transition $^3H_4 \rightarrow {}^1D_2$. (Sample with 0.5 mol%.)

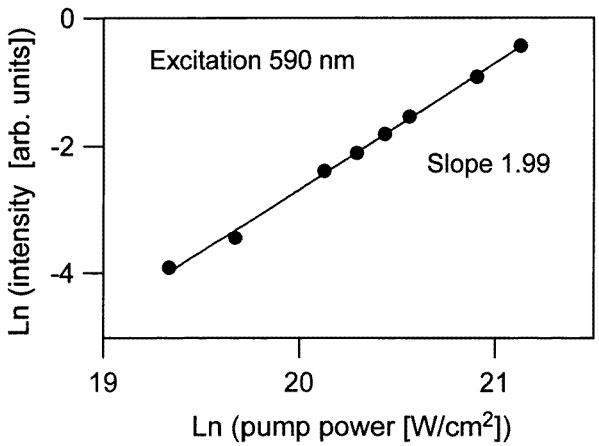

Figure 7. Logarithmic plot of the integrated intensity of the upconverted $^3P_0 \rightarrow {}^3H_4$ emission as a function of the pump laser intensity. Data correspond to 4.2 K and 0.5 mol% of Pr^{3+}.

of the anti-Stokes $^3P_0 \rightarrow {}^3H_4$ emission shows a small rise time ($\approx$0.2 μs), and the lifetime is slightly longer ($\approx$9 μs) than that of the $^3P_0$ level under direct excitation.

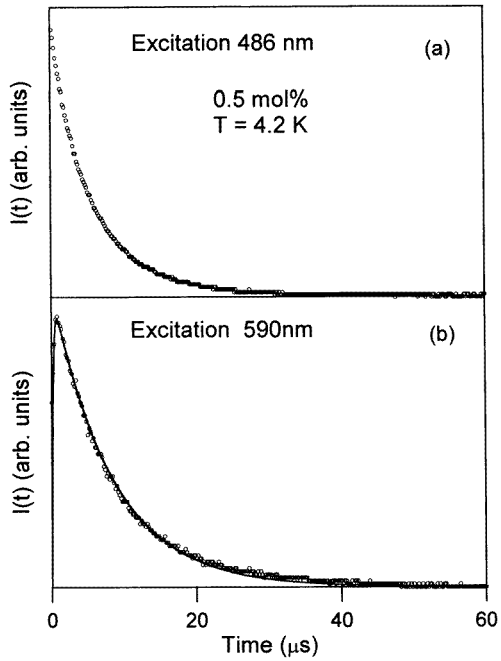

Figure 8. Experimental emission decay curves of level $^3P_0$ obtained (a) under direct excitation (486 nm) and (b) under excitation in resonance with the transition $^3H_4 \rightarrow {}^1D_2$ (590 nm) for the sample doped with 0.5 mol% of Pr^{3+}. Symbols correspond to experimental data and the solid line is the fit to equation (4). Data correspond to 4.2 K.

4. Discussion

The characteristic decay time of the $^1D_2$ state of Pr^{3+} ions should be governed by a sum of probabilities for several competing processes: radiative decay, non-radiative decay by multiphonon emission and by energy transfer to other Pr^{3+} ions. Nonradiative decay by multiphonon emission from the $^1D_2$ level is expected to be small because of the large energy gap to the next lower $^1G_4$ level ($\approx$6950 cm^{-1}) as compared with the highest energies of the phonons involved ($\leqslant$890 cm^{-1}) [6, 22]. Hence, at low temperature and low concentration (0.05 mol%) the measured lifetime, which is single exponential, should approach the radiative lifetime of the $^1D_2$ level. As the concentration rises, the lifetime decreases even at 4.2 K which indicates that Pr–Pr relaxation processes play an important role. Thus the experimental decay time for the sample doped with 0.5 mol% can be written as the sum of the radiative relaxation rate and the energy transfer rate as follows:

$$\frac{1}{\tau_{\exp}} = \frac{1}{\tau_R} + W_{Pr-Pr}. \tag{1}$$

The characteristics of the donor decay time can be discussed in terms of three different regimes: (i) direct relaxation (no diffusion), (ii) diffusion-limited relaxation and (iii) fast diffusion. In the case of fast diffusion, the decay of the donor fluorescence is purely exponential [23]. As we have seen for the sample doped with 0.5% the decays are non-exponential and therefore fast diffusion can be neglected at this concentration. In this sample the decay is

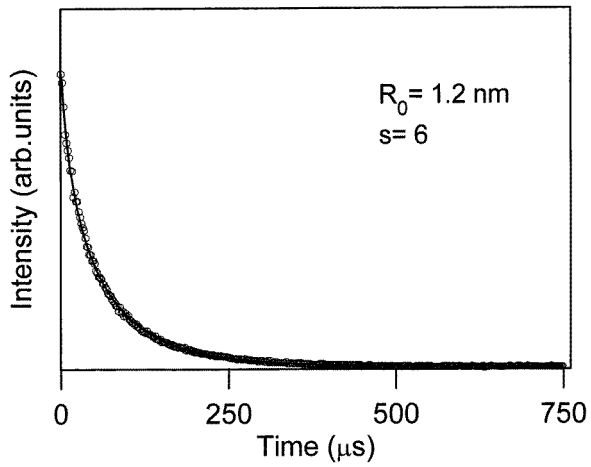

Figure 9. Experimental emission decay curves of $^1D_2$ level and the calculated fit for dipole–dipole interaction ($s = 6$) (solid line) for the sample doped with 0.5 mol% of Pr^{3+} at 4.2 K.

characterized by an initial non-exponential portion followed by an exponential decay governed by the intrinsic decay rate. The initial non-exponential decay is the one attributed to relaxation by direct Pr–Pr energy transfer [23].

Considering the case of direct transfer, for multipolar interactions, the energy transfer probability can be expressed by:

$$W(R) = \frac{1}{\tau_0}\left(\frac{R_0}{R}\right)^s \tag{2}$$

where R_0 is the critical radius defined as the distance at which the energy transfer rate for an isolated donor–acceptor pair is equal to the spontaneous decay rate of the donor τ_0 and s is the parameter of the multipolar interaction ($s = 6$, 8 or 10 for dipole–dipole, dipole–quadrupole and quadrupole–quadrupole interactions respectively). With this transfer probability the donor decay curves can be expressed by the Dexter model [24]:

$$I(t) = I(0)\exp\left\{-\frac{t}{\tau_0} - \Gamma\left(1-\frac{3}{s}\right)\frac{4}{3}\pi R_0^3 N\left(\frac{t}{\tau_0}\right)^{3/s}\right\} \tag{3}$$

where N is the acceptor concentration and $\Gamma(1-3/s)$ is the gamma function. To determine the appropriate multipole interaction we have analysed the measured decay curves for the sample doped with 0.5 mol% of Pr^{3+} with equation (3) taking R_0 as a variable parameter for $s = 6$, 8 and 10. The intrinsic decay time (145 μs) is obtained from the low temperature decay of the less concentrated sample ($x = 0.05$) which is single exponential.

Figure 9 shows a least squares fit of the experimental Pr^{3+} decay at 4.2 K to equation (3) for the sample doped with 0.5 mol%. The best fit obtained was for $s = 6$ with a critical transfer radius $R_0 = 12$ Å. As can be observed, a dipole–dipole transfer mechanism is consistent with the experimental decay intensities. No evidence of diffusion among Pr^{3+} ions was found at this concentration. However, diffusion process could be competitive with a direct transfer at sufficiently high concentrations.

Other energy transfer processes which may contribute to the observed quenching of fluorescence from the $^1D_2$ level are the ones leading to frequency upconversion. Ions in the $^1D_2$ state can upconvert back to the $^3P_0$ giving anti-Stokes fluorescence. The dynamics

of this fluorescence depends on the lifetimes of the levels involved and on the upconversion energy transfer rate. Upconversion by energy transfer leads to a decay curve for the anti-Stokes emission which shows a rise time after the laser pulse, followed by a decay and a lifetime longer than that of the $^3P_0$ level under direct excitation [25].

The decay curves of the anti-Stokes $^3P_0 \rightarrow {}^3H_4$ emission show a certain delay (or rise) time (see figure 8(b)). The observed rise time of the $^3P_0$ decays obtained under pulsed excitation in the $^1D_2$ state indicates that the energy transfer process is responsible for the anti-Stokes fluorescence of Pr^{3+} in these glasses. This process has been observed in borate [15] and fluoroindate [16] glasses and has been attributed to a redistribution of energy between two ions according to: $^1D_2 + {}^1D_2 \rightarrow {}^3P_0 + {}^1G_4$ + phonons.

This process proposed to explain the ETU [26, 27], considers the transfer inside pairs of ions after selective excitation by a pulsed laser. In this model, when both ions of a pair are excited to the $^1D_2$ state, a transfer occurs by which one ion loses energy and goes to the lower excited level $^1G_4$, while the other one gains energy and goes to the $^3P_2$ level from where, by non-radiative decay, the $^3P_0$ level is populated.

The temporal behaviour of the fluorescence can be derived from rate equations for the population density of the pair states involved in the process. By solving the population equations for the doubly excited ion pair, the time evolution of the $^3P_0$ emission after $^1D_2$ excitation is given by:

$$N_3 = \frac{N_d^0 W_t}{W_3 - 2W_2 - W_t}(e^{-(2W_2+W_t)t} - e^{-W_3 t}) \tag{4}$$

where N_d^0 is the number of doubly excited ion pairs just after the laser pulse, W_3, W_2 are the decay rates from $^3P_0$ and $^1D_2$ respectively and W_t is the transfer rate [27]. In this equation, the highest exponent determines the rise of the decay, whereas the lowest one determines the decay. According to equation (4) the rise time of the upconverted emission should be governed by lifetime $1/W_3$ of state $^3P_0$, followed by an exponential decay attributed to the decay of the $^1D_2$ level, W_2, and the transfer rate W_t. However, in this case a short rise time is observed ($\approx 0.2\ \mu$s) which is much shorter than the $^3P_0$ decay time ($\approx 6\ \mu$s). Consequently, the rise time cannot be identified as $1/W_3$. This situation has also been found in LaF_3 [28] and in $YAlO_3$ [29] crystals and attributed to the limitations of the model assumed, i.e. in the concentrated Pr^{3+} systems, $^1D_2$ decay is non-exponential and W_3 values could be different for the specific ion pairs [28].

The fitting of the experimental decay of the upconverted fluorescence to equation (4) is shown in figure 8(b) for the sample doped with 0.5 mol%. The rise and decay times in this case can be assigned to $2W_2 + W_t$ and W_3 respectively. The values of W_3 and W_t deduced by using $W_2 = 6.89 \times 10^3\ s^{-1}$ (the decay rate from $^1D_2$) are $1.2 \times 10^5\ s^{-1}$ and $4.9 \times 10^5\ s^{-1}$ respectively. This analysis suggests that this mechanism for ETU could explain the upconverted fluorescence in this system though some other processes feeding level $^3P_0$ could also occur.

5. Conclusions

From the above results, the following conclusions can be reached:

(i) Fluorescence quenching from the $^1D_2$ state has been demonstrated to occur for Pr^{3+} concentrations higher than 0.05 mol% even at 4.2 K. This can be attributed to a cross relaxation process by analogy with other known Pr-doped materials.

(ii) The time evolution of the decays from the $^1D_2$ state for the sample doped with 0.5 mol% is consistent with a dipole–dipole direct energy transfer mechanism.

(iii) Anti-Stokes fluorescence from the $^3P_0 \rightarrow {}^3H_4$ transition under excitation of the $^1D_2$ level was observed. A rise time was found to be associated with the $^3P_0$ decays showing that this level is populated from lower lying levels and supporting the argument that energy transfer is responsible for the upconversion process. However, this process seems to be complex enough to allow for the use of a single model which could explain the behaviour observed.

Acknowledgments

We would like to thank E Montoya (Departamento de Física de Materiales of the Autonomous University of Madrid) for his assistance with upconversion measurements. This work was supported by the Spanish Government (DGICYT PB95-0512, and CICYT MAT97-1009), the Basque Government (PI97/99) and the Basque Country University (G21/98).

References

[1] Weber M J 1990 *J. Non-Cryst. Solids* **123** 208 and references therein
[2] Blasse G 1985 *J. Less-Common Met.* **112** 1
[3] Verweij H and Buster J H J M 1979 *J. Non-Cryst. Solids* **34** 81
[4] Ribeiro S J L, Dexpert-Ghys J, Piriou B and Mastelaro V R 1993 *J. Non-Cryst. Solids* **159** 213
[5] Canale J E, Condrate R A, Nassau K Sr and Cornilsen B C 1986 *J. Can. Ceram. Soc.* **55** 50
[6] Wang J, Lincoln J R, Brocklesby W S, Deol R S, Mackechnie C J, Pearson A, Tropper A C, Hanna D C and Payne D N 1993 *J. Appl. Phys.* **73** 8066
[7] Lezal D, Pedlíková J and Horák J 1996 *J. Non-Cryst. Solids* **196** 178
[8] Kaminskii A A 1991 *Ann. Phys., Paris* **16** 639
[9] Allain J Y, Monerie M and Poignant H 1991 *Electron. Lett.* **27** 1156
[10] Smart R G, Hanna D C, Tropper A C, Davey S T, Carter S F and Szebesta D 1991 *Electron. Lett.* **27** 1307
[11] Remilleux A and Jacquier B 1996 *J. Lumin.* **68** 279
[12] Johnson L F and Guggenheim H J 1971 *Appl. Phys. Lett.* **19** 44
[13] Joubert M F, Guy S and Jacquier B 1993 *Phys. Rev.* B **48** 10 031
[14] Capobianco J A, Raspa N, Monteil A and Malinowski M 1993 *J. Phys.: Condens. Matter* **5** 6083
[15] Pacheco E M and de Araujo C B 1988 *Chem. Phys. Lett.* **148** 334
[16] de Araujo L E E, Gomes A S L and de Araujo C B 1994 *Phys. Rev.* B **50** 16 219
[17] Kim S Il and Yun S I 1994 *J. Lumin.* **60/61** 233
[18] Balda R, Fernández J, Adam J L, Mendioroz A and Arriandiaga M A 1999 *J. Non-Cryst. Solids* at press
[19] Dornauf H and Heber J 1980 *J. Lumin.* **22** 1
[20] Hegarty J, Huber D L and Yen W M 1982 *Phys. Rev.* B **25** 5638
[21] de Mello Donegá C, Lambaerts H, Meijerink A and Blasse G 1993 *J. Phys. Chem. Solids* **54** 873
[22] Pan Z, Morgan S H, Dyer K, Ueda A and Liu H 1996 *J. Appl. Phys.* **79** 8906
[23] Weber M J 1971 *Phys. Rev.* B **4** 2932
[24] Dexter D L 1953 *J. Chem. Phys.* **21** 836
[25] Malta O L, Anti-Fidancev E, Lemaitre-Blaise M, Dexpert-Ghys and Piriou B 1986 *Chem Phys. Lett.* **129** 557
[26] Zalucha D J, Wright J C and Fong F K 1973 *J. Chem. Phys.* **59** 997
[27] Buisson B and Vial J C 1981 *J. Physique Lett.* **42** L115
[28] Vial J C, Buisson R, Madeore F and Poirier M 1979 *J. Physique* **40** 913
[29] Malinowski M, Garapon C, Joubert M F and Jaquier B 1995 *J. Phys.: Condens. Matter* **7** 1995